Correspondence to:
S. Wang,
shuai.wang@imperial.ac.uk

A Shortening of the Life Cycle of Major Tropical Cyclones

S. Wang[1] [ID], **T. Rashid[1,2], H. Throp[1], and R. Toumi[1]**

[1]Department of Physics, Imperial College London, London, UK, [2]Department of Epidemiology and Biostatistics, School of Public Health, Imperial College London, London, UK

Abstract In this study a comprehensive picture of the changing intensity life cycle of major (Category 3 and higher) tropical cyclones (TCs) is presented. Over the past decades, the lifetime maximum intensity has increased, but there has also been a significant decrease in duration of time spent at intensities greater than Category 1. These compensating effects have maintained a stable global mean-accumulated cyclone energy of individual major TCs. The global mean duration of major TCs has shortened by about 1 day from 1982 to 2018. There has been both faster intensification (Categories 1 to 3) and weakening (Categories 3 to 1) by about 40%. The probabilities of rapid intensification and rapid weakening have both risen in the period 2000–2018 compared to 1982–1999. A statistically significant anticorrelation is found between the lifetime maximum intensity and the following duration of the final weakening. This suggests an element of self-regulation of TC life cycles.

Plain Language Summary The destructive potential of tropical cyclones (TCs) is conventionally represented by the maximum wind speed near the surface, known as the TC intensity. The intensity life cycle —from intensification to maturity to weakening—is a fundamental feature of TCs. A good understanding of the complete TC intensity life cycle is of vital importance to evaluate their impacts. This study presents a comprehensive picture of the changing intensity life cycle of strong TCs with relatively high intensity. The total duration of these potentially high-impact TCs has been shortened by about 1 day from 1982 to 2018, which is mainly due to faster early intensification and final weakening. Based on previous studies, a more rapid early intensification could be linked to anthropogenic forcing. It is more likely for a TC with higher intensity during its whole life span to experience a more rapid final weakening, which appears to be an element of self-regulation of TC life cycles, whereby a high maximum core intensity sows the seeds for a faster weakening.

1. Introduction

A fundamental property of tropical cyclones (TCs) is the intensity life cycle, measured conventionally by the near-surface maximum wind speed (V_m). A TC intensity life cycle can be decomposed into four stages: genesis, intensification, maturity, and weakening/transition (Dunn & Miller, 1960; Riehl, 1954; Simpson & Riehl, 1981). The lifetime maximum intensity (LMI), the maximal turning point of the intensity time series, has been extensively studied for decades (e.g., Camargo & Sobel, 2005; Chan et al., 2001; DeMaria, 1996; Elsner et al., 2008; Emanuel et al., 2004). The potential upper limit of LMI, known as the maximum potential intensity, is proposed based on environmental conditions (Emanuel, 1995; Holland, 1997).

The time scale to reach LMI from genesis is determined by the intensification rate. Emanuel (2000) found that the mean intensification rate in the North Atlantic (NA) is $12 \, \mathrm{m \, s^{-1} \, day^{-1}}$. A consistent rate was also found at a global level (Wang & Toumi, 2018). The intensification rate is determined by a combination of internal and environmental factors, for example, the current intensity, maximum potential intensity, vertical wind shear, atmospheric convective instability, and upper-ocean thermal stratification (DeMaria, 2009, 1996; Emanuel et al., 2004). Kishtawal et al. (2012) showed a significant increase in the intensification rate of global TCs, except in the Western Pacific (WP). Bhatia et al. (2019) confirmed this finding in the NA and linked the change to anthropogenic forcing.

The weakening stage following the LMI has received much less attention (Colomb et al., 2019; Ma et al., 2019; Wood & Ritchie, 2015). This is somewhat surprising and anomalous since the weakening phase lasts for a similar length of time as intensification and is also more likely to occur close to land than over the open ocean and thus is important to understanding impact. A TC weakens when the environmental
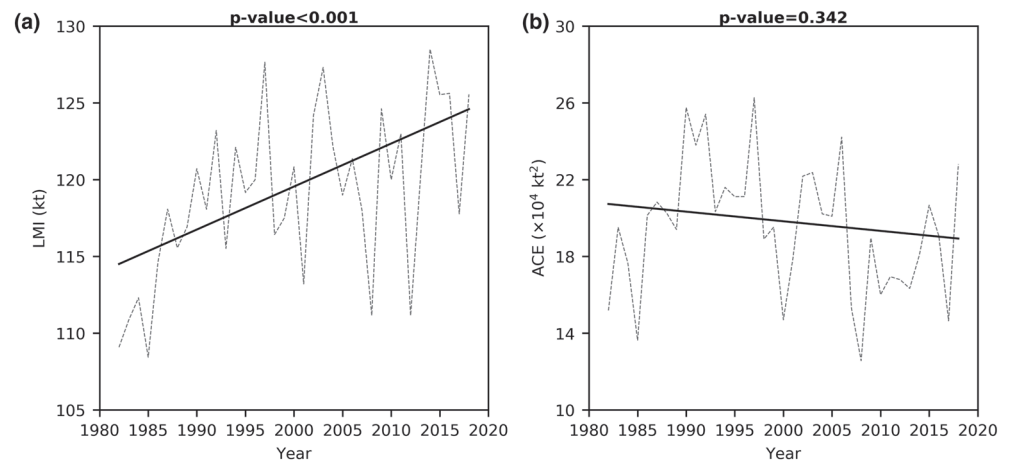
Figure 1. Global trends of annual mean (a) lifetime maximum intensity (LMI) and (b) accumulated cyclone energy (ACE) for major TCs in the period 1982–2018. The linear trends, calculated with the weighted linear regression based on annual sample numbers, are shown in thick lines. The two-sided p value of the trend from weighted linear regression is provided using the Wald test with t distribution of the test statistic.

conditions become unfavorable. This usually happens when a TC loses enthalpy flux from the warm ocean by, for example, moving to higher latitudes and/or experiencing rapid energy dissipation during landfall. Any trends in the duration of weakening stage currently remain unexplored. The objective of this study is to provide a more comprehensive picture of the recent changes in the complete TC intensity life cycle. We will show that the mean total duration of major TCs has become significantly shorter, which is mainly due to both faster early intensification and final weakening. The next section presents data sources and methods. The main results are located in section 3, followed by discussion and conclusions in the last section.

2. Methods

The best track data set are taken from the International Best Track Archive for Climate Stewardship (IBTrACS, Version 4.0). The National Hurricane Center provides the best track records in the NA and Eastern Pacific (EP), and the best track data from the Joint Typhoon Warning Center are used in the WP, North Indian Ocean (NI), South Indian Ocean (SI), and South Pacific (SP). The analysis is conducted in the period 1982–2018 when the global TC record is more completely monitored by satellites (Kossin et al., 2014). We focus on major TCs—Category 3 (CAT 3) and above based on the Saffir-Simpson Hurricane Scale (Simpson & Saffir, 1974).

The duration of four periods in terms of intensity evolution will be analyzed, including the following:

1. **CAT 1→3**: an early intensification from CAT 1 to CAT 3 (V_m from 64 to 96 kts).
2. **CAT 3→1**: a final weakening from CAT 3 to CAT 1 (V_m from 96 to 64 kts).
3. **CAT 3→3**: the period between the early intensification and final weakening when the intensity is maintained as at least CAT 3 (V_m from 96 to 96 kts).
4. **CAT 1→1**: the total duration from the moment of reaching CAT 1 in the early intensification period to the moment of weakening to CAT 1 in the final weakening phase (V_m from 64 to 64 kts).

The following data filters are applied in sequence for preprocessing:

1. Only the TCs with an LMI of at least CAT 3 (i.e., major TCs) are kept.
2. Only the records at standard reporting times are considered, that is, 00, 06, 12, and 18 UTC.
3. For each case, only the records from the last CAT 1 point prior to LMI and the first point post LMI are included.
4. For each case, no landfall, defined as the moment when a TC center moves into land, is allowed during the selected period.
5. Only the TCs that have the period CAT 1→1 completely within the latitude band 40°N to 40°S are kept.
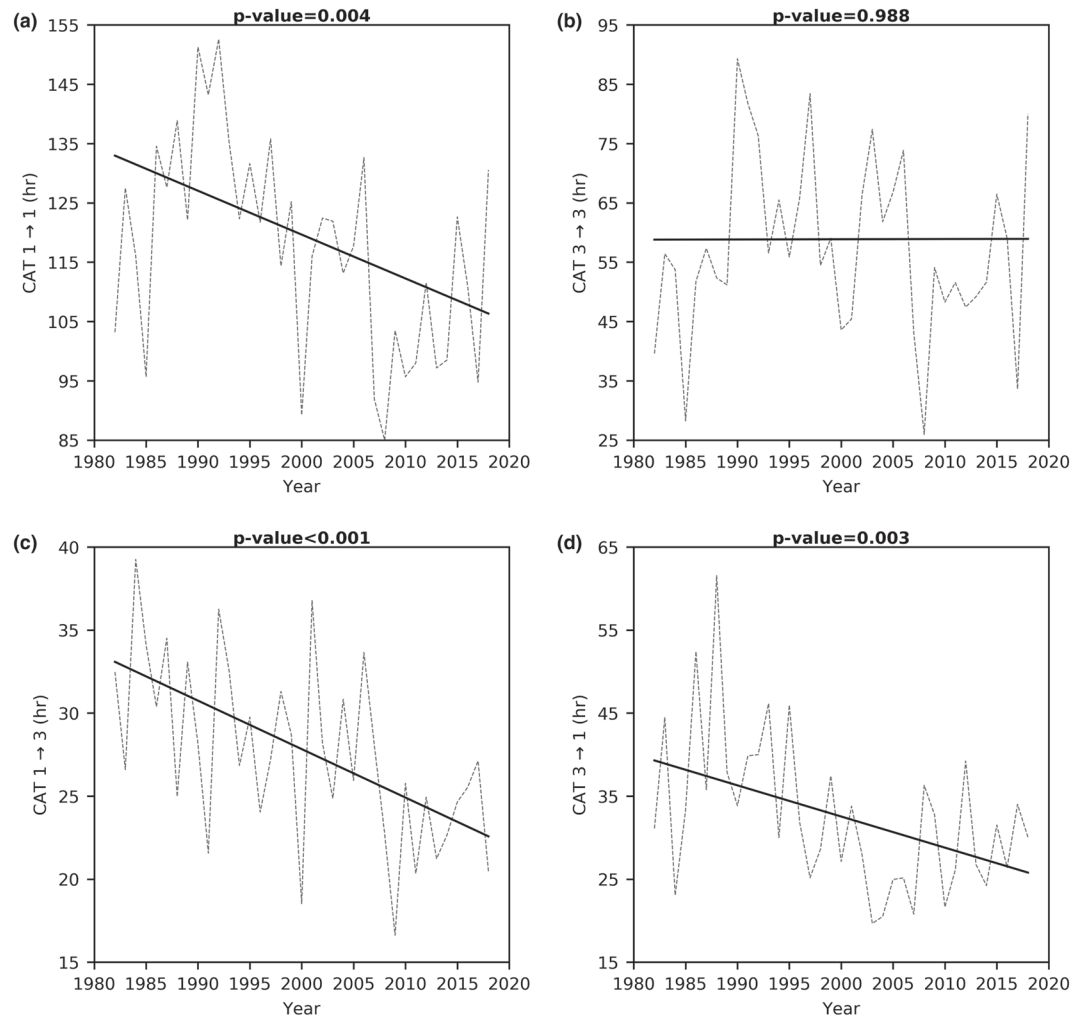
Figure 2. As in Figure 1, but for the duration of (a) total period (CAT1→1), (b) major TC period (CAT3→3), (c) early intensification (CAT1→3), and (d) final weakening (CAT3→1).

After the filtering, there are 24, 160, 162, 5, 113, and 64 cases left in the NA, EP, WP, NI, SI, and SP, respectively. This accounts for 61% of all global major TCs for 1982–2018.

3. Results

Figure 1a shows that from 1982 to 2018, the global mean LMI of major TCs has increased by 10 kts, with a statistically significant trend of 3 kts per decade ($p<0.001$). Different from the LMI, which is based singularly on a peak intensity at one time, the accumulated cyclone energy (ACE, Bell et al., 2000) is widely used as a metric for representing TC activity, convolving both the intensity and duration information. We find a nonsignificant decline (-0.5×10^4 kt^2 per decade, $p=0.342$) of average TC ACE for period spent above CAT 1 (Figure 1b).

Figure 2a shows that the duration of CAT 1→1 has reduced by a significant rate of −6% (−7 hr) per decade ($p=0.004$) relative to the global annual mean for 1982–2018. This negative trend is not due to any duration change of the time spent as a major TC (CAT 3→3) (Figure 2b). The shortening of the intensity life cycle is partly due to a shorter time of early intensification, CAT 1→3, of −10% (−3 hr) per decade ($p<0.001$; Figure 2c). However, there is also a significant downward trend of duration for the weakening period, CAT 3→1, with a rate of −11% (−4 hr) per decade ($p=0.003$; Figure 2d). Figure 2 illustrates that during
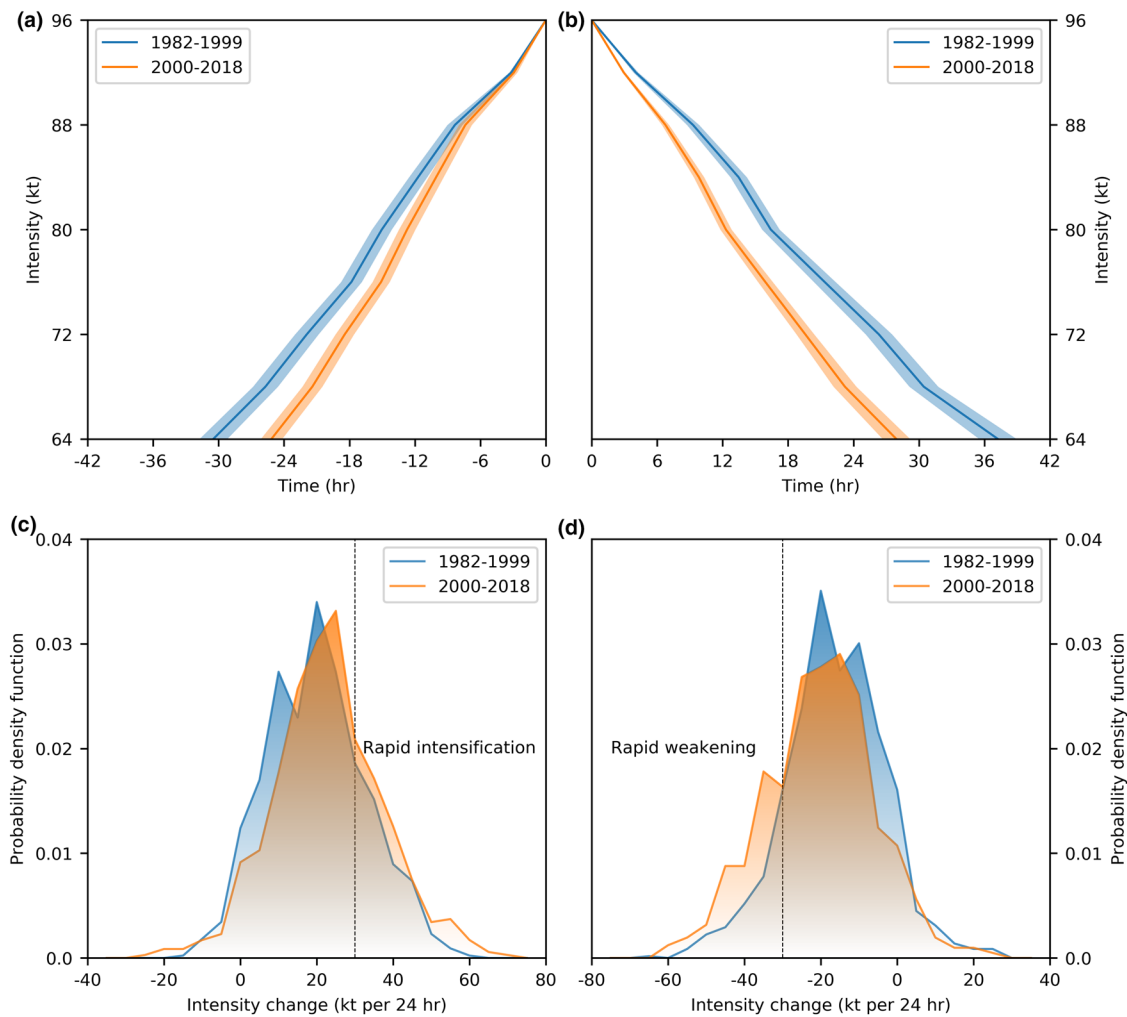
Figure 3. Changes in intensity evolution in (a and c) early intensification and (b and d) final weakening before and after 2000. (a and b) Intensity composites were calculated by linearly interpolating the intensity change of each TC between 64 and 96 kt with an interval of 4 kt. The shadings in (a) and (b) represent the standard error of the mean. (c and d) Observed 24 hr intensity change was calculated with a bin width of 5 kt.

1982–2018, the average major TC intensity life cycle has been shortened by about 1 day, due to reduced duration of both early intensification and final weakening by about 40%.

We break down TC intensity life cycle into three parts with the times of intensity changing to CAT 3, rather than other intensity levels. This choice has a physical reason since we focus on dangerous major TCs whose LMI must go above this threshold. The complete picture of intensity life-cycle change is established with six trend analyses shown in Figures 1 and 2. Although our approach is a planned comparison because the intensity thresholds are meaningful, it may be argued that these six tests could be considered as a family of multiple comparisons. Even after applying a Bonferroni correction (adjusting the significant level to $0.05/6 \approx 0.01$ for each trend), the detected trends remain significant at the 95% confidence interval.

If the TCs with landfall are included (in which case 96% of all major TCs are used for the calculation), the duration trends of CAT 1→1, 1→3, and 3→1 are −4% per decade ($p=0.021$), −9% per decade ($p<0.001$), and −9% per decade ($p=0.006$), respectively (1–2% weaker than the trends with the landfall filter). A similar analysis for major TCs was also conducted for the full intensification period from CAT 1 to LMI and the weakening period from LMI to the moment when intensity drops below CAT 1. There is no significant trend found for the full intensification period ($p=0.100$) at the 95% confidence interval, but a shortening of the full weakening period can still be detected (−7% per decade, $p=0.016$). When we include both minor and major TCs in the analysis, neither full intensification nor weakening period shows any significant duration trend.

Table 1
Mean Relative Changes (%) of Lifetime Maximum Intensity (LMI) and the Duration of Four Intensity Evolution Periods in the Second Epoch (2000–2018) Compared to the Mean in the First Epoch (1982–1999) of Global and the Northern Hemisphere (NH), Southern Hemisphere (SH), North Atlantic (NA), Eastern Pacific (EP), Western Pacific (WP), South Indian Ocean (SI), and South Pacific (SP) Major TCs

	Global	NH	SH	NA	EP	WP	SI	SP
CAT 1 → 3	**−17**	**−18**	−15	**−54**	**−22**	−9	**−21**	−2
	[−28, −7]	[−31, −6]	[−32, 2]	[−87, −21]	[−41, −4]	[−30, 10]	[−43, 0]	[−26, 23]
CAT 3 → 1	**−25**	**−21**	**−33**	−19	−21	**−24**	**−28**	**−41**
	[−36, −14]	[−35, −7]	[−52, −16]	[−72, 28]	[−44, 2]	[−40, −8]	[−52, −5]	[−68, −16]
CAT 3 → 3	−7	−11	6	−29	−8	−11	3	11
	[−19, 5]	[−27, 4]	[−14, 25]	[−83, 23]	[− 32, 18]	[−29, 8]	[−21, 27]	[−22, 43]
CAT 1 → 1	**−11**	**−17**	−1	**−34**	**−20**	−6	−2	1
	[−19, −4]	[−26, −8]	[−13, 12]	[−61, −7]	[−34, −6]	[−19, 7]	[−18, 15]	[−19, 21]
LMI	**6**	3	**11**	−1	1	**8**	**8**	**15**
	[3, 9]	[−1, 7]	[6, 16]	[−10, 9]	[−4, 6]	[2, 14]	[2, 15]	[6, 23]

Note. The statistics are not calculated separately in the North Indian Ocean (NI) due to limited sample size but included in the global calculation. Significance is denoted in bold at 95% confidence interval with a two-sided bootstrapping method. The two tested distributions were resampled by 100,000 times to generate 100,000 pairs of distributions with the same sample size as its parent distribution. The mean difference of each pair was then calculated to form a new distribution with 100,000 samples. We extracted the 2.5th and 97.5th percentiles of the new distribution from the last step as the 95% confidence interval bounds given in the square brackets.

We next continue the analysis by dividing the 37 years into two epochs: 1982–1999 and 2000–2018. The early intensification and final weakening composites show clear epochal changes in duration (Figures 3a and 3b). Figures 3c and 3d show that in the second epoch, there is an increased probability of rapid intensification (weakening) defined as an intensity change of more than ±30 kts per 24 hr (Kaplan & DeMaria, 2003; Wood & Ritchie, 2015). Figure 3 suggests almost mirror-like intensity changes between the early intensification and final weakening periods.

The duration changes in all basins are shown in Table 1. For the early intensification period, CAT 1→3, the TCs in the NA, EP, and SI have a significantly shorter duration in the second epoch. For the final weakening, CAT 3→1, duration shortening is significant in the WP, SI, and SP. For the major TC period, CAT 3→3, none of the basins have experienced any detectable duration change. For the total period, CAT 1→1, NA, and EP TCs show significant duration shortening. It is interesting to note that every basin with a significant LMI increase also shows a detectable duration shortening of the final weakening. This supports an overall negatively correlated relationship between the two.
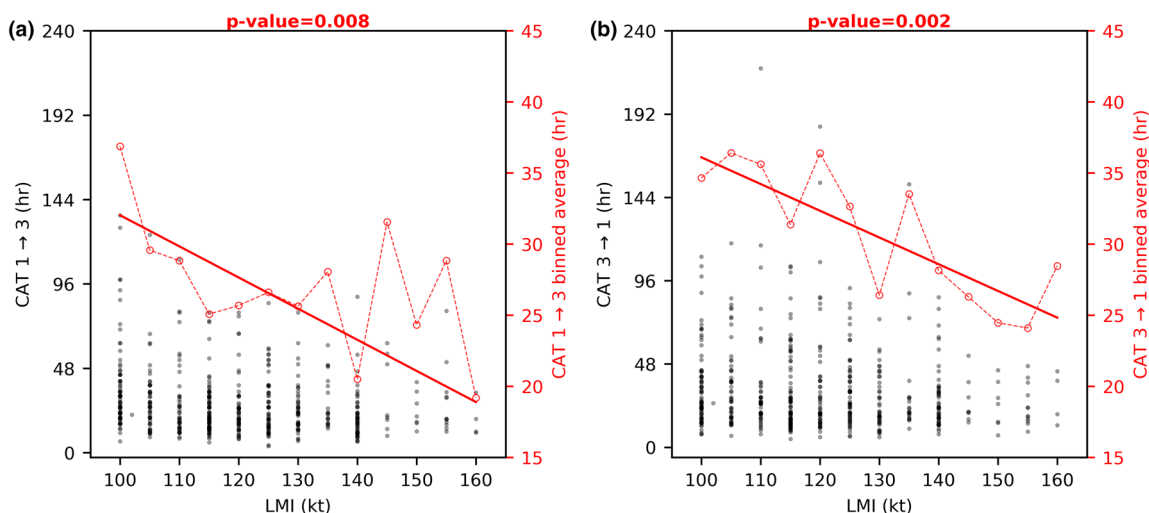
Figure 4. Comparison between lifetime maximum intensity (LMI) and the duration of (a) early intensification (CAT1→3) and (b) final weakening (CAT3→1) of global major TCs. Each black dot represents one case. The mean durations in each 5 kt intensity bin are shown by the red dots. The linear fit of binned average duration with respect to LMI is denoted by the thick red line with the weighted linear regression based on the sample size in each bin. The fitted slope is −0.22 and −0.19 hr per kt for intensification and weakening, respectively.

Figure 4b shows a significant sensitivity of CAT 3→1 duration to LMI with a slope of −0.19 hr per kt (p=0.002). A significant anticorrelation is also found between the period of early intensification and LMI (−0.22 hr per kt, p=0.008; Figure 4a). To test the influence of any potential outlier, the significance of the anticorrelation is reproduced by leaving one reading out of the calculation. For the intensification, only when the binned duration at 100 kt is kept does the anticorrelation remain significant ($p \leq 0.05$). By contrast, the weakening anticorrelation is always significant in all tested combinations with a p value of at least 0.01. Apart from a smaller p value as shown in Figure 4b, this calculation also emphasizes the robustness of the negative relationship between the LMI and the duration of final weakening.

4. Discussion and Conclusions

Our analysis with the best track data reveals that the LMI shows a significant upward trend in the period 1982–2018 for major TCs (LMI of CAT 3 or greater). Also based on the best track data, Webster (2005) found a more than 50% of increase in the frequency of CAT 4 and 5 TCs in 1990–2004 compared to the number in 1975–1989. However, it was questioned by Klotzbach and Landsea (2015), who noted observational improvements causing temporal inhomogeneities in the somewhat subjective best track data. Using an objectively satellite-derived TC intensity data set covering 1981–2006, Elsner et al. (2008) found a significant upward trend of LMI in global major TCs with a rate of about 3 kts per decade (converted with the trend at the 0.8 quantile in their Figure 1b), which is in line with the LMI trend as reported here (3 kts per decade) but with the best track data.

We have shown that both the early intensification and final weakening periods of major TCs have become shorter. Bhatia et al. (2019) found rising probability in both high (intensification) and low (weakening) tails of the rate of 24 hr intensity changes. Recent higher probability of rapid intensification, as shown in Figure 3, agrees with their study, attributing the changes to anthropogenic forcing. Kang and Elsner (2019) found that the proportion of WP TCs experiencing rapid intensification has increased by 30% in the past 30 years. Rapid intensification is likely to lead to a higher LMI (Lee et al., 2016), and this could be one reason for the anticorrelation between the duration of CAT 1→3 and LMI in Figure 4a. The upward trend of global LMI in Figure 1a could therefore be expected with more rapid intensification events in recent decades.

The rising probability of rapid weakening was left unexplored in Bhatia et al. (2019). Our study takes one step forward by demonstrating that rapid intensification and rapid weakening have been more frequent concurrently. Dramatic intensity changes account for an important error source of TC intensity forecast (Elsberry et al., 2007; Emanuel et al., 2016; Kaplan et al., 2010). The TC intensity life-cycle changes reported here may bring extra challenges to TC intensity predictability. Ma et al. (2019) found almost constant 24 hr weakening rate above an initial intensity of Category 3 or higher. Their definition of weakening includes fluctuations above CAT 3 (e.g., from CAT 4 to 3 within 24 hr) and is thus different, as it does not consider the final decay to CAT 1 as we explicitly consider here.

The causes of the enhanced weakening rate remains to be found. Weakening happens once, for example, the frictional dissipation is no longer balanced by sufficient surface heat fluxes, or a stronger vertical shear distorts the vortex and vertical heating. The frictional boundary layer spin-down explanation does not seem to explain the higher weakening rate, as the intensity at the beginning of the final weakening period is the same in all cases (Category 3). Land influence is also unlikely to be an explanation since the trends are even stronger when excluding landfall. Lower SSTs can promote weakening (Walker et al., 2014), but a systemic change would not be consistent with known widespread ocean warming. Weakening may be promoted by faster translation speed (Ma et al., 2019), but that would also not be consistent with a recently reported global slowdown of TC movement by Kossin (2018), which is however disputed (Chan, 2019; Yamaguchi et al., 2020). Increased vertical wind shear (Wood & Ritchie, 2015) and more midlevel dry air intrusion (Colomb et al., 2019) are other unproven candidates for more rapid weakening process.

We speculate that one of the reasons for the recent faster weakening is that TCs with higher peak intensity also create the thermodynamic conditions for speeding up the weakening. There is a consensus that the convective available potential energy (CAPE) decreases from outer wind radii toward the TC center due to core intensification (e.g., Bogner et al., 2000). TC intensity and the inner core CAPE are interdependent. High CAPE favors initial intensification, but higher intensity at a later stage is associated with lower CAPE in

the core, which is depressed by past stronger convection (Nguyen et al., 20114). The TC with a higher LMI will have a larger radial gradient of CAPE. The strongest convection could migrate away from the core. Outward migration of the eyewall would reduce the inertial stability, thus enabling stronger mass inflow. This increases the positive pressure tendency in the TC core, reduces the low-level pressure gradient near the core, and hastens the maximum surface wind speed decline. This hypothesis will be examined in more detail in further work. Based on the observational analysis presented in this study, there appears to be a plausible self-regulation of TC life cycle, whereby a high maximum core intensity sows the seeds for increased weakening.

Data Availability Statement

The tropical cyclone best track data used in this study can be downloaded from the IBTrACS website (https://www.ncdc.noaa.gov/ibtracs/index.php?name=ib-v4-acces).

References

Bell, G. D., Halpert, M. S., Schnell, R. C., Higgins, R. W., Lawrimore, J., Kousky, V. E., et al. (2000). Climate Assessment for 1999. *Bulletin of the American Meteorological Society*, *81*(6), s1–s50.

Bhatia, K. T., Vecchi, G. A., Knutson, T. R., Murakami, H., Kossin, J., Dixon, K. W., & Whitlock, C. E. (2019). Recent increases in tropical cyclone intensification rates. *Nature Communications*, *10*(1), 1–9. https://doi.org/10.1038/s41467-019-08471-z

Bogner, P. B., Barnes, G. M., & Franklin, J. L. (2000). Conditional instability and shear for six hurricanes over the Atlantic Ocean. *Weather and Forecasting*, *15*(2), 192–207. https://doi.org/10.1175/1520-0434(2000)015<0192:CIASFS>2.0.CO;2

Camargo, S. J., & Sobel, A. H. (2005). Western North Pacific tropical cyclone intensity and ENSO. *Journal of Climate*, *18*(15), 2996–3006. https://doi.org/10.1175/JCLI3457.1

Chan, K. T. F. (2019). Are global tropical cyclones moving slower in a warming climate? *Environmental Research Letters*, *14*(10), 104015. https://doi.org/10.1088/1748-9326/ab4031

Chan, J., Duan, Y., & Shay, L. K. (2001). Tropical cyclone intensity change from a simple ocean-atmosphere coupled model. *Journal of the Atmospheric Sciences*, *58*(2), 154–172. https://doi.org/10.1175/1520-0469(2001)058<0154:TCICFA>2.0.CO;2

Colomb, A., Kriat, T., & Leroux, M. D. (2019). On the rapid weakening of very intense tropical Cyclone Hellen (2014). *Monthly Weather Review*, *147*(8), 2717–2737. https://doi.org/10.1175/MWR-D-18-0309.1

DeMaria, M. (1996). The effect of vertical shear on tropical cyclone intensity change. *Journal of the Atmospheric Sciences*, *53*(14), 2076–2088. https://doi.org/10.1175/1520-0469(1996)053<2076:TEOVSO>2.0.CO;2

DeMaria, M. (2009). A simplified dynamical system for tropical cyclone intensity prediction. *Monthly Weather Review*, *137*(1), 68–82. https://doi.org/10.1175/2008MWR2513.1

Dunn, G. E., & Miller, B. I. (1960). *Atlantic hurricanes*. Baton Rouge, LA: Louisiana State University Press.

Elsberry, R. L., Lambert, T. D. B., & Boothe, M. A. (2007). Accuracy of Atlantic and Eastern North Pacific tropical cyclone intensity forecast guidance. *Weather and Forecasting*, *22*(4), 747–762. https://doi.org/10.1175/WAF1015.1

Elsner, J. B., Kossin, J. P., & Jagger, T. H. (2008). The increasing intensity of the strongest tropical cyclones. *Nature*, *455*(7209), 92–95. https://doi.org/10.1038/nature07234

Emanuel, K. (1995). Sensitivity of tropical cyclones to surface exchange coefficients and a revised steady-state model incorporating eye dynamics. *Journal of the Atmospheric Sciences*, *52*(22), 3969–3976.

Emanuel, K. (2000). A statistical analysis of tropical cyclone intensity. *Monthly Weather Review*, *128*(4), 1139–1152.

Emanuel, K., DesAutels, C., Holloway, C., & Korty, R. (2004). Environmental control of tropical cyclone intensity. *Journal of the Atmospheric Sciences*, *61*(7), 843–858.

Emanuel, K., Zhang, F., Emanuel, K., & Zhang, F. (2016). On the predictability and error sources of tropical cyclone intensity forecasts. *Journal of the Atmospheric Sciences*, *73*(9), 3739–3747. https://doi.org/10.1175/JAS-D-16-0100.1

Holland, G. J. (1997). The maximum potential intensity of tropical cyclones. *Journal of the Atmospheric Sciences*, *54*(21), 2519–2541.

Kang, N. Y., & Elsner, J. B. (2019). Influence of global warming on the rapid intensification of western North Pacific tropical cyclones. *Environmental Research Letters*, *14*(4), 044027. https://doi.org/10.1088/1748-9326/ab0b50

Kaplan, J., & DeMaria, M. (2003). Large-scale characteristics of rapidly intensifying tropical cyclones in the North Atlantic basin. *Weather and Forecasting*, *18*(6), 1093–1108. https://doi.org/10.1175/1520-0434(2003)018<1093:LCORIT>2.0.CO;2

Kaplan, J., DeMaria, M., & Knaff, J. A. (2010). A revised tropical cyclone rapid intensification index for the Atlantic and eastern North Pacific basins. *Weather and Forecasting*, *25*(1), 220–241. https://doi.org/10.1175/2009WAF2222280.1

Kishtawal, C. M., Jaiswal, N., Singh, R., & Niyogi, D. (2012). Tropical cyclone intensification trends during satellite era (1986-2010). *Geophysical Research Letters*, *39*, L10810. https://doi.org/10.1029/2012GL051700

Klotzbach, P. J., & Landsea, C. W. (2015). Extremely intense hurricanes: Revisiting Webster et al. (2005) after 10 years. *Journal of Climate*, *28*(19), 7621–7629. https://doi.org/10.1175/JCLI-D-15-0188.1

Kossin, J. P. (2018). A global slowdown of tropical-cyclone translation speed. *Nature*, *558*(7708), 104–107. https://doi.org/10.1038/s41586-018-0158-3

Kossin, J. P., Emanuel, K. A., & Vecchi, G. A. (2014). The poleward migration of the location of tropical cyclone maximum intensity. *Nature*, *509*(7500), 349–52.

Lee, C.-Y., Tippett, M. K., Sobel, A. H., & Camargo, S. J. (2016). Rapid intensification and the bimodal distribution of tropical cyclone intensity. *Nature Communications*, *7*(1), 10625. https://doi.org/10.1038/ncomms10625

Ma, Z., Fei, J., & Huang, X. (2019). A definition of rapid weakening for tropical cyclones over the Western North Pacific. *Geophysical Research Letters*, *46*, 11,471–11,478. https://doi.org/10.1029/2019GL085090

Nguyen, M. C., Reeder, M. J., Davidson, N. E., Smith, R. K., & Montgomery, M. T. (2014). Inner-core vacillation cycles during the intensification of Hurricane Katrina. *Quarterly Journal of the Royal Meteorological Society*, *137*(657), 829–844. https://doi.org/10.1002/qj.823

Riehl, H. (1954). *Tropical meteorology*. New York: McGraw-Hill.

Simpson, R. H., & Riehl, H. (1981). *The hurricane and its impact*. Baton Rouge, LA: Louisiana State University Press.

Simpson, R. H., & Saffir, H. (1974). The hurricane disaster potential scale. *Weatherwise*, *27*(8), 169.

Walker, N. D., Leben, R. R., Pilley, C. T., Shannon, M., Herndon, D. C., Pun, I. F., et al. (2014). Slow translation speed causes rapid collapse of northeast Pacific Hurricane Kenneth over cold core eddy. *Geophysical Research Letters*, *41*, 7595–7601. https://doi.org/10.1002/2014GL061584

Wang, S., & Toumi, R. (2018). A historical analysis of the mature stage of tropical cyclones. *International Journal of Climatology*, *38*(5), 2490–2505. https://doi.org/10.1002/joc.5374

Webster, P. J. (2005). Changes in tropical cyclone number, duration, and intensity in a warming environment. *Science*, *309*(5742), 1844–1846.

Wood, K. M., & Ritchie, E. A. (2015). A definition for rapid weakening of North Atlantic and eastern North Pacific tropical cyclones. *Geophysical Research Letters*, *42*, 10,091–10,097. https://doi.org/10.1002/2015GL066697

Yamaguchi, M., Chan, J. C. L., Moon, I. J., Yoshida, K., & Mizuta, R. (2020). Global warming changes tropical cyclone translation speed. *Nature Communications*, *11*(1), 1–7. https://doi.org/10.1038/s41467-019-13902-y